Tumor Microenvironment

Blockade of a Chemokine, CCL2, Reduces Chronic Colitis-Associated Carcinogenesis in Mice

Boryana Konstantinova Popivanova,[1] Feodora Ivanova Kostadinova,[1] Kengo Furuichi,[2] Mohamed M. Shamekh,[1] Toshikazu Kondo,[4] Takashi Wada,[3] Kensuke Egashira,[5] and Naofumi Mukaida[1]

[1]Division of Molecular Bioregulation, Cancer Research Institute and Departments of [2]Disease Control and Homeostasis and [3]Laboratory Medicine, Graduate School of Medical Sciences, Kanazawa University, Kanazawa, Japan; [4]Department of Forensic Medicine, Wakayama Medical University, Wakayama, Japan; and [5]Department of Cardiovascular Medicine, Graduate School of Medical Sciences, Kyushu University, Fukuoka, Japan

Abstract

Accumulating evidence indicates the crucial contribution of chronic inflammation to various types of carcinogenesis, including colon carcinoma associated with ulcerative colitis and asbestosis-induced malignant mesothelioma. Ulcerative colitis–associated colon carcinogenesis can be recapitulated in mice by azoxymethane administration followed by repetitive dextran sulfate sodium ingestion. In the course of this carcinogenesis process, the expression of a macrophage-tropic chemokine, CCL2, was enhanced together with intracolonic massive infiltration of macrophages, which were a major source of cyclooxygenase (COX)-2, a crucial mediator of colon carcinogenesis. Mice deficient in CCL2-specific receptor, CCR2, exhibited less macrophage infiltration and lower tumor numbers with attenuated COX-2 expression. Moreover, CCL2 antagonists decreased intracolonic macrophage infiltration and COX-2 expression, attenuated neovascularization, and eventually reduced the numbers and size of colon tumors, even when given after multiple colon tumors have developed. These observations identify CCL2 as a crucial mediator of the initiation and progression of chronic colitis–associated colon carcinogenesis and suggest that targeting CCL2 may be useful in treating colon cancers, particularly those associated with chronic inflammation. [Cancer Res 2009;69(19):7884–92]

Introduction

Ulcerative colitis (UC) is a major form of inflammatory bowel disease (IBD), an immune-mediated chronic intestinal condition (1). The major symptom of UC is bloody mucoid diarrhea and its clinical course is characterized by repetitive relapses and remissions. Pathologic features of UC include prominent leukocyte infiltration in the colonic mucosa and uncontrolled and prolonged inflammatory reactions (1). These conditions frequently cause epithelial dysplasia and DNA damage with microsatellite instability, and eventually can progress to cancer (2). Indeed, involvement of entire colon for longer than 10 years predisposes UC patients to colon cancer (2), indicating the essential contribution of chronic inflammation to colon carcinogenesis. Thus, to develop measures to prevent cancer development in UC patients, it is necessary to gain an understanding of the pathogenesis of UC at molecular and cellular levels. Moreover, evidence is accumulating that chronic inflammatory conditions also can cause cancer in other organs as observed on asbestosis and silicosis (3). Thus, elucidation of colon carcinogenesis in UC will also shed a novel light on chronic inflammation-associated carcinogenesis in general.

Oral administration of dextran sulfate sodium (DSS) to rodents is widely used to recapitulate human UC, because it can induce pathologic changes similar to that observed in UC patients (4). Moreover, repeated oral DSS ingestion can cause colon carcinoma (5) and this carcinogenesis process is promoted by a prior administration of azoxymethane (AOM), which causes O^6-methyl-guanine formation (6). Activation of NF-κB pathway contributes to this colon carcinogenesis by preventing colon epithelial cell apoptosis and promoting growth factor production by inflammatory cells (7). The crucial involvement of NF-κB activation in colon carcinogenesis prompted us to investigate the roles of the tumor necrosis factor (TNF)-α/TNF receptor axis, because TNF-α is abundantly expressed in colon of patients with IBD (8), and is one of major target molecules of NF-κB and a major activator of NF-κB (9). We showed that combined treatment with AOM and DSS induced the intracolonic expression of TNF-α, which in turn regulates the trafficking of macrophages and granulocytes, major sources of cycolooxygenase (COX)-2, thereby resulting in the development and progression of colon cancer (10).

TNF-α lacks direct chemotactic activities for macrophages and granulocytes, but can induce the expression of various chemokines in several cell types present in colon tissues such as epithelial cells, fibroblasts, endothelial cells, and leukocytes (9). Thus, it is likely that enhanced TNF-α expression in colon tissues can induce the expression of chemokines active on macrophages and granulocytes. Indeed, the mucosa of patients with IBD exhibited enhanced mRNA and protein expression of MCP-1/CCL2 (11–13), a C-C chemokine with potent chemotactic and activating activities for monocytes/macrophages (14). We previously consistently observed that combined treatment of AOM and DSS enhanced CCL2 mRNA expression in colon tissues and that blocking the TNF-α/TNF receptor axis reduced colorectal carcinogenesis, intracolonic macrophage infiltration, and CCL2 mRNA expression (10). These observations prompted us to

investigate the roles of the interaction between CCL2 and its specific receptor, CCR2, in colon carcinogenesis induced by the combined treatment with AOM and DSS. By using CCR2-deficient mice and CCL2 blocking agents, we here document that CCL2 interactions with CCR2 have vital roles in the initiation and progression of colitis-associated colon carcinogenesis.

Materials and Methods

Reagents and antibodies. AOM and DSS (MW 36,000–50,000) were purchased from Sigma-Aldrich, Inc. and MP Biomedicals, Inc., respectively. A specific CCR2 antagonist, propagermanium, was kindly provided by Sanwa Chemical Co. Human CCL2 NH_2-terminal deleted form 7ND-expressing vector was prepared by cloning human CCL2 NH_2-terminal– deleted cDNA with an epitope FLAG tag in the carboxyl terminal portion to the pcDNA3 expression vector as described previously (15). Rat monoclonal anti-F4/80 antibody was obtained from Serotec. Goat polyclonal anti–COX-2 and mouse monoclonal anti-cytokeratin 20 antibodies were obtained from Santa Cruz Biotechnology and Abcam, respectively. Rabbit polyclonal anti–β-catenin and mouse monoclonal ANTI-FLAG M2 antibodies were from Sigma-Aldrich, Inc. Rat monoclonal anti-CD31 antibody was from BD Biosciences Pharmingen. Rabbit polyclonal anti-CCL2 and anti-CCR2 antibodies were prepared by immunizing rabbits with mouse CCL2 protein and CCR2 peptide as previously described (16).

Animal experiments. Pathogen-free 8- to 12-wk-old female wild-type BALB/c mice (WT) and CCR2-deficient mice, on a BALB/c genetic background, were housed under specific pathogen-free conditions with free access to food and water during the course of experiments. Mice were injected i.p. with 12 mg/kg body weight of AOM dissolved in physiologic saline. Five days later, 2% DSS was given in the drinking water over 5 d, followed by 16 d of regular water. This cycle was repeated a total of thrice. Body weights were measured every week and the animals were sacrificed at the indicated time intervals for macroscopic inspection, histologic analysis, and total RNA extraction. In some experiments, 7ND-expressing or pcDNA3 vector was injected into the femoral muscle of WT mice at day 56. Immediately after the injection, a pair of electrode pads was inserted onto the muscle to encompass the injected site, and electrical pulses were delivered six times (100V, 50-ms pulse) with an electrical pulse generator (ECM830, BTX). At 11 d after the transfection, reverse transcription-PCR detected 7ND gene expression selectively in muscle of mice receiving 7ND-expressing vector (Supplementary Fig. S1*A*). Moreover, immunohistochemical analysis detected 7ND protein in the muscle of WT mice receiving 7ND-expressing vector, but not those receiving pcDNA3 vector (Supplementary Fig. S1*B*). In another series of experiments, WT mice were given propagermanium at a dose of 8 mg/kg body weight, mixed with the food, every day from day 56 to day 60. All animal experiments were performed in compliance with the Guideline for the Care and Use of Laboratory Animals of Kanazawa University.

Bone marrow chimeric mice generation. Cell suspensions from male WT or CCR2-deficient bone marrow were prepared from femurs and tibias, filtered, and counted. Female WT or CCR2-deficient mice received a single i.v. injection of 1×10^7 bone marrow cells, after being irradiated with 4.25 Gy X-rays followed by 4.25 Gy X-rays (MPR-1520R, Hitachi) 4 h later. The following groups of chimeric mice were generated: WT to WT, WT to CCR2 deficient, CCR2 deficient to WT, and CCR2 deficient to CCR2 deficient mice. To verify successful reconstitution of bone marrow in recipient mice, genomic DNA was extracted from peripheral blood. Quantitative PCR was performed to detect *Sry* gene present in the Y chromosome (forward, 5′-TGGGACTGGTGACAATTGTC-3′; reverse, 5′-CTCTGTATTTTGCATG-CATGCTGG-3′) and *GAPDH* gene as an internal control with the help of Fast SYBR Green Master mix (Qiagen) as described previously (17). We calculated the chimeric rates on the assumption that the ratio of *Sry* to *GAPDH* gene was 100% in male mice. We confirmed that the rates of WT to CCR2-deficient and CCR2-deficient to WT mice were 97.6 ± 2.4% and 84.2 ± 5.0%. After bone marrow reconstitution was confirmed, mice were given sequentially with AOM and DSS as described above.

Histopathologic and immunohistochemical analyses of mouse colon tissues. Resected mouse colon tissues were fixed in 10% formalin neutral buffer solution (Wako) for paraffin embedding or were immediately frozen in Tissue-Tek ornithine carbamyl transferase compound (Sakura Fine Technical Co.) and stored at −80°C. Paraffin-embedded sections were cut at 5 μm and stained with H&E solution. Paraffin-embedded sections were additionally deparaffinized for immunohistochemical detection of β-catenin–, CCR2-, CCL2-, F4/80-, Ly-6G–, COX-2-, cytokeratin 20–, and FLAG-positive cells. Frozen sections were used for immunohistochemical detection of mouse CD31-positive cells. Endogenous peroxidase activity was blocked using 3% H_2O_2 for 5 min, followed by incubation with Non-Specific Staining Blocking reagent (DakoCytomation) for 10 min. The sections were incubated with the optimal dilutions of anti-CCR2, anti-CCL2, anti-F4/80, anti-CD3, anti–β-catenin, anti–COX-2, anti-CD31, anti-cytokeratin 20, or anti-FLAG antibodies overnight at 4°C. β-Catenin– and CCR2-positive cells were detected with horseradish peroxidase–labeled anti-rabbit polymer (EnVision+ System, DakoCytomation), whereas F4/80-positive cells were detected using Catalyzed Signal Amplification System (DakoCytomation). Immune complexes were visualized with Peroxidase Substrate 3,3′-diaminobenzidine (DAB) kit (Vector Laboratories, Inc.). CCL2-, COX-2–, and CD31-positive cells were detected by the incubation with anti-rabbit, anti-goat, or anti-rat biotinylated IgG (DakoCytomation; dilution, 1:200). Detection of cytokeratin 20 and FLAG tag was performed with Vector M.O.M. Immunodetection kit (Vector Laboratories, Inc.), according to the manufacturer's instructions. The resultant immune complexes were visualized by ABC *Elite* kit (Vector Laboratories, Inc.) and Peroxidase Substrate DAB kit (Vector Laboratories, Inc.) according to the manufacturer's instructions. Finally, the slides were counterstained with hematoxylin, dehydrated, and coverslipped. Positive cells were enumerated on five randomly chosen visual fields at ×400 magnification. The pixel numbers of CD31-positive areas were measured on five randomly chosen visual fields at ×200 magnification with the aid of Adobe Photoshop software.

A double-color immunofluorescence analysis. Colon tissues were processed to a double-color immunofluorescence analysis using the combination of anti-CCR2 and anti-COX–2 antibodies. Alexa Fluor 488 donkey anti-rabbit and Alexa Fluor 546 donkey anti-goat antibodies were used as secondary antibodies. Immunofluorescence was visualized on a Carl Zeiss Laser Scanning Microscope 510.

RT-PCR analysis. Total RNA was extracted from colon or muscle tissues with RNeasy Mini kit (Qiagen) and 2.5 μg of RNA was reverse transcribed using ReverTraAce and random primers as described previously (10). Thereafter, 2 μL of resultant cDNA was used to amplify 7ND and *GAPDH* gene using Taq DNA polymerase and 10 μmol/L of specific sets of primers with the predetermined optimal cycle consisting of 94°C for 30 s, 55°C for 1 min, and 72°C for 1 min (Supplementary Table S1) as described previously. The PCR products were fractionated on 1.5% agarose gel and visualized by ethidium bromide staining. Real-time PCR was performed on Applied Biosystems StepOne Real-Time PCR System using the comparative C_T quantitation method. TaqMan Gene Expression Assays (Applied Biosystems), containing specific primers and TaqMan MGB probe (FAM dye-labeled), TaqMan Fast Universal PCR Master Mix were used with 10 ng of cDNA to detect and quantify the expression levels of CCL2 and COX-2 in mouse colon tissues. Glyceraldehyde-3-phosphate dehydrogenase (GAPDH) was amplified as internal control. C_T values of GAPDH were subtracted from C_T values of the target genes (ΔC_T). ΔC_T values of treated mice were compared with ΔC_T values of untreated animals. Reactions were done at 95°C, 20 s, then 95°C, 00:01, 60°C, 20 s, 40 cycles.

DNA sequencing and mutation analysis of *β-catenin* gene. Genomic DNA was extracted from tumor tissues obtained from WT mice receiving either 7ND-expressing or pcDNA3 vector by using NucleoSpin Tissue kit (Macherey-Nagel, Inc.) according to the manufacturer's instructions. Exon 3 of the *β-catenin* gene, containing the consensus sequence for glycogen synthase kinase-3β phosphorylation, was amplified by PCR, using specific primers (forward, 5′-GCTGACCTGATGGAGTTGGA-3′; reverse, 5′-GCTACTTGCTCTTGCGTGAA-3′) and the following thermal cycling parameters: 35 cycles of 94°C, 5 min; followed by 94°C, 45 s, 55°C, 1 min, 72°C, 1 min; followed by 72°C, 5 min. PCR products were subcloned into
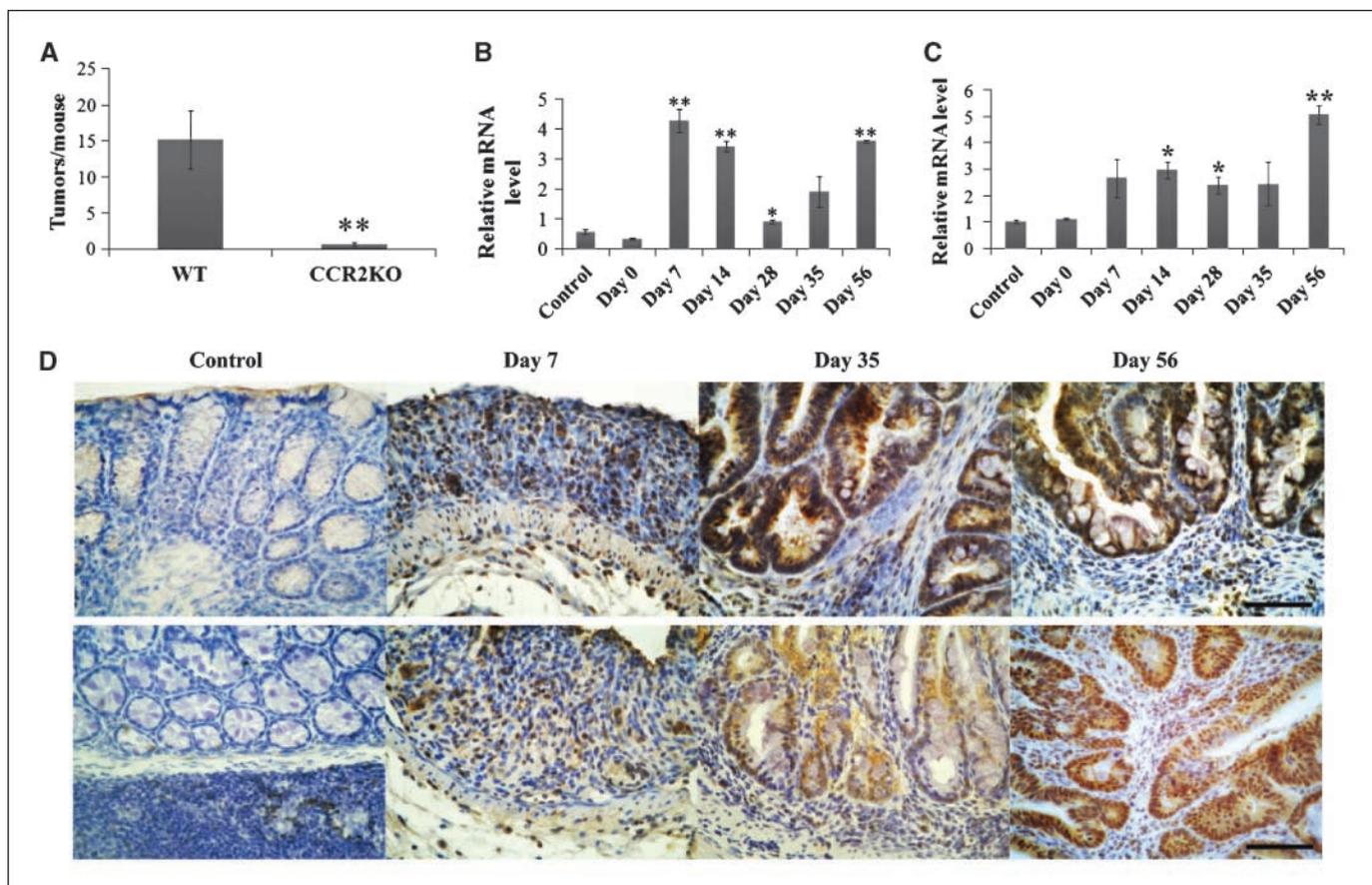
Figure 1. Tumor formation in WT and CCR2-deficient (*CCR2KO*) mice after AOM and DSS treatment. *A,* tumor numbers. Colons were removed at day 56 to determine the numbers of macroscopic tumors. *Columns,* mean (*n* = 10 animals); *bars,* SD. **, *P* < 0.01 versus WT mice. *B, CCL2* gene expression in the colons of WT mice. The levels of *CCL2* mRNA were quantified by real-time RT-PCR as described in Materials and Methods, and normalized to the level of GAPDH mRNA. *, *P* < 0.05; **, *P* < 0.01 versus untreated (*control*) mice. *C, CCR2* gene expression in the colons of WT mice. The levels of *CCR2* mRNA were quantified by real-time RT-PCR as described in Materials and Methods, and normalized to the level of GAPDH mRNA. *, *P* < 0.05; **, *P* < 0.01 versus untreated (*control*) mice. *D,* immunohistochemical detection of CCL2-positive (*top*) and CCR2-positive cells (*bottom*) in the colons. Colons were obtained from WT mice at the indicated time points. Immunohistochemical analysis was conducted as described in Materials and Methods. Representative results from five independent animals are shown here. *Scale bars,* 50 μm.

pSTBlue-1 vector (AccepTor vector, Novagen) and sequenced using BigDye Terminator Ver. 3.1 Cycle Sequencing kit (Applied Biosystems) on an ABI PRISM 3100-*Avant* Genetic Analyzer (Applied Biosystems).

Statistical analysis. The mean ± SD were calculated for all parameters determined. Statistical significance was evaluated using one-way ANOVA, and *P* values lower than 0.05 were considered statistically significant.

Results

Enhanced CCL2 expression in the colon during the course of colon carcinogenesis. Consistent with our previous observations (10), a single i.p. injection of the carcinogen AOM, followed by three rounds of 2% DSS intake, induced the development of multiple tumors from the middle to distal colon of WT mice (Supplementary Fig. S2; Fig. 1*A*). Because we previously observed a massive macrophage infiltration during the whole course of this colon carcinogenesis process, we investigated the expression of a macrophage-tropic chemokine MCP-1/CCL2 and its single specific receptor, CCR2. *CCL2* mRNA expression level was negligible in untreated WT mice and immediately after AOM treatment, but subsequent to DSS administration, *CCL2* mRNA expression was augmented with a fluctuation (Fig. 1*B*). Similarly, *CCR2* mRNA level was enhanced in WT mice after DSS intake (Fig. 1*C*) but *CCR2*

mRNA could not be detected in CCR2-deficient mice under the present experimental conditions (data not shown). CCL2 protein was detected in mononuclear cells, particularly macrophages, infiltrating the lamina propria and submucosal regions, and also in endothelial cells at the earlier phase and colon carcinoma cells at the later phase (Fig. 1*D, top*). Immunohistochemical analysis showed that CCR2 was expressed by mononuclear cells infiltrating in the lamina propria and submucosal regions of the colon, and by some colon carcinoma cells during the course of colon carcinogenesis (Fig. 1*D, bottom*).

Reduction in AOM/DSS-induced inflammatory reaction and subsequent tumor formation in the absence of CCR2. A massive infiltration of CCR2-positive cells prompted us to investigate the roles of the CCL2-CCR2 interactions in this colon carcinogenesis. There were no apparent differences in macroscopic and microscopic appearance of the colon of untreated WT and CCR2-deficient mice (Fig. 2*A*). When both strains were treated with AOM and DSS, WT mice exhibited marked body weight loss and bloody diarrhea, whereas CCR2-deficient mice showed a minimal body weight loss and diarrhea (data not shown). In WT mice, multiple tumors extended from most of the middle to distal colon by day 56, whereas the numbers and sizes of tumors were remarkably reduced

in the colons of CCR2-deficient mice even at day 56 (Supplementary Fig. S2; Fig. 1A). Microscopic analysis consistently showed that WT mice developed severe inflammation with massive infiltration of leukocytes into the mucosa, submucosal edema, and loss of entire crypts and surface epithelium, particularly in the middle to distal colon at day 7 (Fig. 2A). At day 14, inflammatory cell infiltration persisted, accompanied with dysplastic glands with hyperchromatic nuclei, decreased mucin production, and dystrophic goblet cells. Moreover, immunohistochemical analysis showed that inflammatory cells consisted of F4/80-positive macrophages (Fig. 2C). AOM treatment most frequently causes mutations of β-catenin and eventually constitutive activation of the Wnt signaling pathway (18). These molecular changes are mirrored by nuclear accumulation of β-catenin in tumor cells. Indeed, at days 28 to 35, adenocarcinomatous lesions exhibited nuclear β-catenin

accumulation together with macrophage and granulocyte infiltration, and their sizes and numbers increased progressively, thereafter (Fig. 2A and B). On the contrary, CCR2-deficient mice displayed only mild inflammatory changes in the colon during the course of DSS administration as evidenced by attenuated infiltration of macrophages (Fig. 2C) and eventually developed only a small number of adenocarcinomatous lesions with less nuclear β-catenin accumulation (Fig. 2A and B). These observations identified the CCL2-CCR2 interactions as crucial for the development of chronic inflammation-associated colon carcinoma.

Contribution of CCR2-expressing bone marrow–derived cells to colon carcinogenesis. CCR2 is expressed by nonbone marrow as well as bone marrow–derived cells (19, 20), and we observed CCR2 expression on some cancer cells. Hence, we compared the contribution of CCR2-expressing nonbone
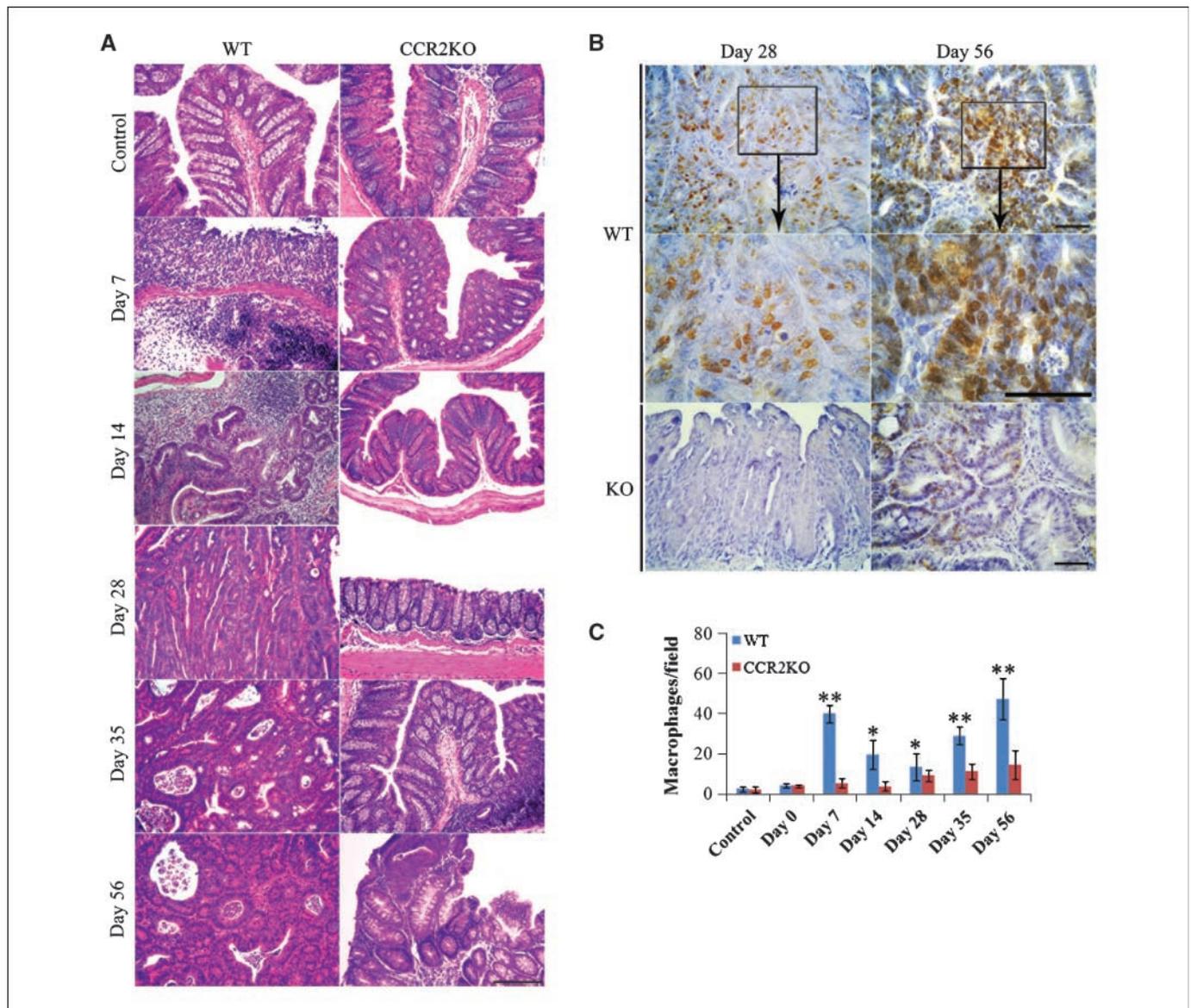

Figure 2. Microscopic analysis of colon tissues. *A,* colons were removed at the indicated time intervals, fixed, and stained with H&E. Representative results from five mice are shown here. *B,* immunohistochemical staining for β-catenin. Colons were removed at the indicated time intervals from WT and CCR2-deficient mice and immunostained with anti–β-catenin antibody as described in Materials and Methods. Representative results from five mice are shown. *C,* the numbers of F4/80-positive cells were counted as described in Materials and Methods and are shown. *Columns,* mean (*n* = 10 animals); *bars,* SD; *, *P* < 0.05; **, *P* < 0.01 versus untreated (*control*) mice. *Scale bars,* 50 μm (*A*) and 20 μm (*B*).

marrow– and bone marrow–derived cells to this colon carcinogenesis by using bone marrow chimeric mice prepared from WT and CCR2-deficient mice. Upon combined treatment with AOM and DSS, CCR2-deficient and WT mice transplanted with WT mouse–derived bone marrow cells developed tumors with a similar incidence, but at a much higher level than either WT or CCR2-deficient mice transplanted with CCR2-deficient mouse–derived bone marrow (Fig. 3). These observations would indicate that CCR2-expressing bone marrow–derived cells, but not nonbone marrow–derived cells were mainly responsible for tumor development in this model.

Reduction in AOM/DSS-induced expression of COX-2 in CCR2-deficient mice. *COX-2* mRNA expression and COX-2–expressing cell number were increased in WT mice following 7 days after the initiation of DSS treatment (Fig. 4A–C) as we previously observed (10). We did not observe any positive staining when we used an isotype IgG instead of anti–COX-2 antibody (data not shown), confirming the specificity of this antibody. In line with our previous observation that COX-2 was expressed by F4/80-positive macrophages, double-color immunofluorescence analysis revealed that the cells that expressed CCR2 also expressed COX-2 (Fig. 4D). AOM/DSS-induced increases in *COX-2* mRNA expression and COX-2–positive cell numbers were decreased in the absence of CCR2 (Fig. 4A–C). Collectively, AOM/DSS failed to increase the expression of COX-2, an enzyme that is crucially involved in colon carcinoma development, in CCR2-deficient mice.

Reduction of tumor formation by CCR2 antagonist administration. To further delineate the role of the CCL2-CCR2 interactions in the progression phase of this colon carcinogenesis model, we administered two distinct types of CCR2 antagonists, 7ND-expressing vector and propagermanium, after three cycles of DSS intake, when multiple colon tumors have developed. When mice were treated with 7ND-expressing vector, the numbers and sizes of macroscopic tumors were markedly reduced (Fig. 5A and B). Histopathologic analysis showed that treatment with 7ND-expressing vector attenuated adenocarcinomatous changes

Figure 3. Colon tumor formation in bone marrow chimeric mice. Bone marrow chimeric mice were generated and subjected to AOM and DSS treatment as described in Materials and Methods. Colons were removed at day 56 and the tumor numbers were determined macroscopically. *Bars,* the mean of each group; each symbol represents the tumor numbers of each animal (*n* = 4–5); *, *P* < 0.05; **, *P* < 0.01; *NS,* not significant.

(Fig. 5C). Likewise, propagermanium treatment reduced the numbers and sizes of tumors and attenuated adenocarcinomatous changes (Supplementary Fig. S3A–C). Concomitantly, treatment with 7ND-expressing vector (Fig. 5D) or propagermanium (Supplementary Fig. S3D) decreased the numbers of infiltrating macrophages. 7ND administration reduced intracolonic COX-2 mRNA expression and COX-2–expressing cell numbers (Supplementary Fig. S4A; Fig. 6A). Moreover, 7ND treatment decreased intratumoral CD31-positive vascular areas significantly (Supplementary Fig. S4B; Fig. 6B). Similarly, reductions in COX-2 expression and intratumoral vascular areas were observed with propagermanium treatment (Supplementary Figs. S5 and S6). Furthermore, 7ND treatment decreased nuclear accumulation of β-catenin in the tumor cells (Supplementary Fig. S4C; Fig. 6C) and the numbers of cytokeratin 20–positive cells (Supplementary Fig. S4C; Fig. 6D). Likewise, propagermanium treatment decreased both β-catenin nuclear accumulation in the tumor cells and cytokeratin 20–positive cell numbers (Supplementary Fig. S7). Finally, the incidence of *β-catenin* mutations was significantly reduced by 7ND treatment (Supplementary Table S2). Collectively, these observations would indicate that CCL2-CCR2 interactions were also crucially involved in the tumor progression phase after multiple tumors developed, by regulating COX-2–expressing macrophage infiltration.

Discussion

CCL2 was originally identified as a chemokine, which is chemotactic for monocytes and macrophages (14). Although most chemokines can bind several distinct receptors with similar affinities, CCL2 uses CCR2 as its single specific receptor (21). Subsequent studies have unraveled the crucial roles of the CCL2-CCR2 interactions in various chronic inflammatory conditions characterized by a macrophage infiltration, such as crescentic glomerulonephritis (22), pulmonary hypertension (23), pulmonary fibrosis (24), atherosclerosis (25), multiple sclerosis (26), and rheumatoid arthritis (27). Moreover, *CCL2* mRNA and protein expression was augmented in the mucosa of patients with IBD (11–13). In a recent study, administration of the antioxidant N-acetyl-ʟ-cysteine to UC patients had beneficial effects together with down-regulation of CCL2 expression levels (28). DSS administration augmented *CCL2* mRNA expression with a fluctuation in the course of colon carcinogenesis. This may mirror the observations that CCL2 protein was detected in macrophages and that the macrophage numbers fluctuated in the course of colon carcinogenesis process. Moreover, genetic deletion of CCR2 protected mice from DSS-induced acute inflammatory changes as previously reported (29). Thus, the CCL2-CCR2 interactions can initiate colon carcinogenesis by inducing inflammation in the colon.

In addition to hematopoietic cells such as macrophages, CCR2 is also expressed by nonhematopoietic cells such as endothelial cells (30), fibroblasts (31), and mesenchymal stem cells (32). In line with the previous observation that CCR2 is expressed by prostate cancer cells (33), we detected CCR2 expression on some cancer cells as well as by infiltrating mononuclear cells in this model. However, the analysis of bone marrow chimeric mice revealed that bone marrow–derived CCR2-expressing but not nonbone marrow–derived cells are indispensable for this colon carcinogenesis, although contribution of bone marrow–derived endothelial progenitor cells (34) and/or fibrocytes (35) cannot be completely excluded.
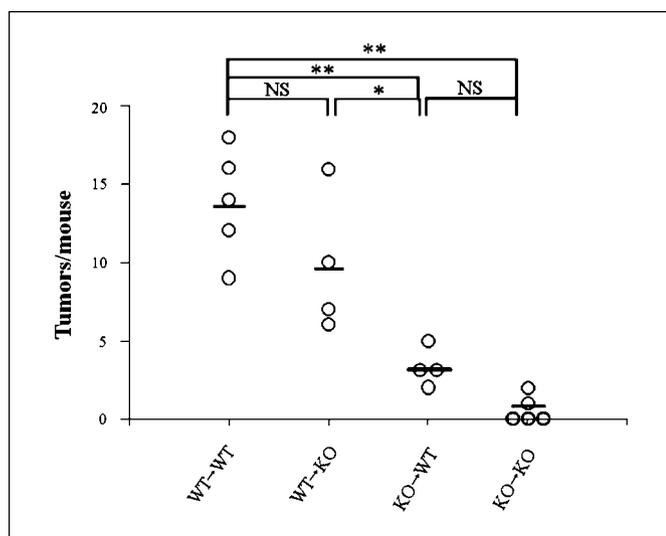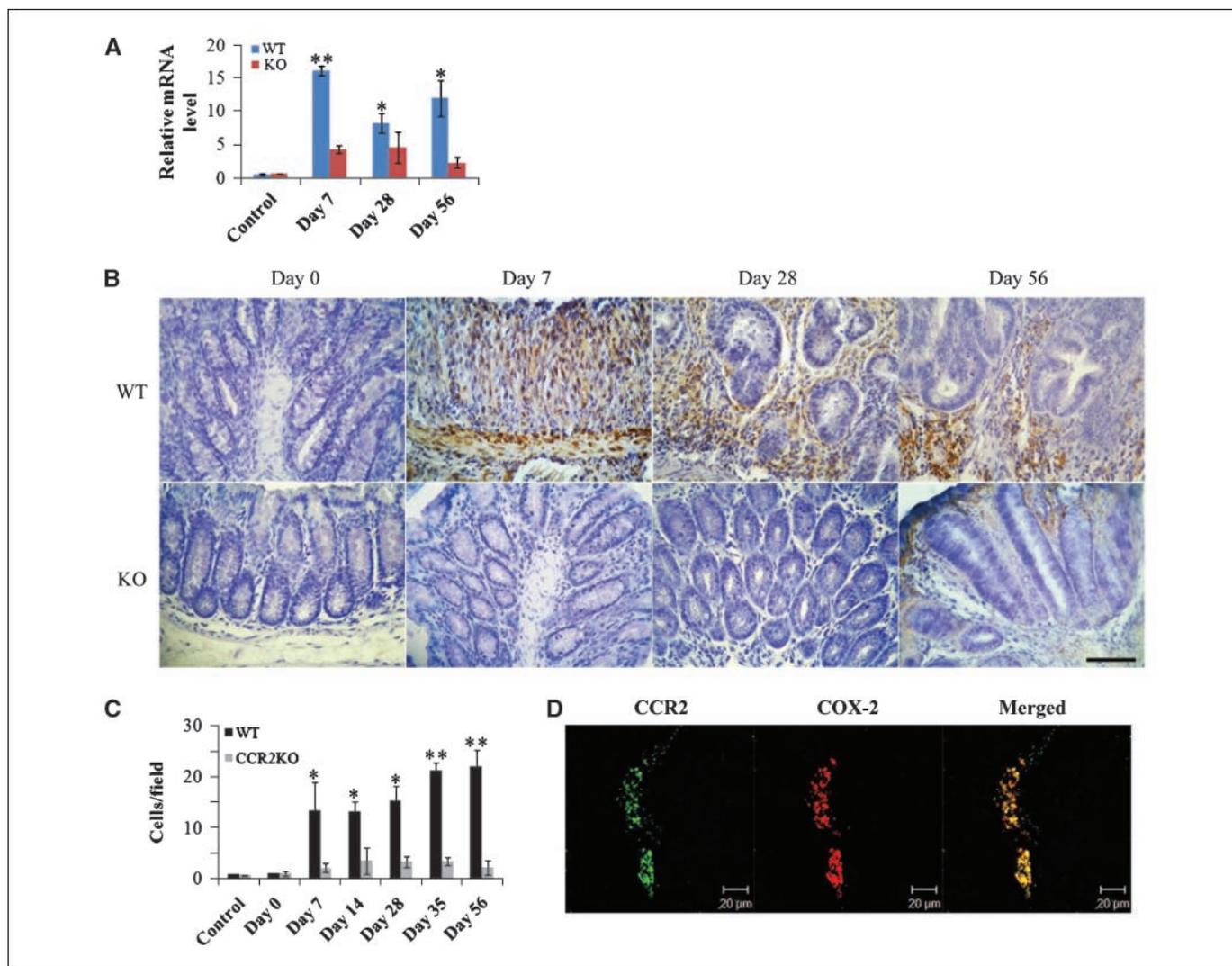
Figure 4. COX-2 expression in the colons. *A,* quantitative RT-PCR was performed on total RNAs extracted from the colons at the indicated time points as described in Materials and Methods. The levels of *COX-2* mRNA were normalized to the levels of *GAPDH* mRNA. *, $P < 0.05$; **, $P < 0.01$ versus untreated mice. *B* and *C,* immunohistochemical detection of COX-2–expressing cells. Colons were obtained from WT mice at the indicated time points and immunostained with anti–COX-2 antibody as described in Materials and Methods. *B,* representative results from six independent animals. The numbers of COX-2–expressing cells were determined. *Columns,* mean; *bars,* SD (*C*). *, $P < 0.05$; **, $P < 0.01$ versus untreated mice. *D,* a double-color immunofluorescence analysis on COX-2 expression by CCR2-expressing cells. Colons were obtained from WT mice and immunolabeled with anti-CCR2 (*left*) and anti–COX-2 antibodies (*middle*). Fluorescence was digitally merged in the right. Representative results from six independent experiments are shown here. *Scale bars,* 20 μm (*B* and *D*).

Andreas and colleagues (29) claimed that upon DSS treatment, CCR2- or CCR5-deficient mice exhibited reduced acute colitis, but with similar level of macrophage infiltration as WT mice. On the contrary, combined blockade of CCR2, CCR5, and CXCR3 protected mice from DSS-induced colitis along with a reduction in intracolonic infiltration of CD11b-positive macrophages (36). We also observed that macrophage infiltration was markedly reduced in CCR2-deficient mice after DSS treatment, compared with WT mice. Moreover, intracolonic macrophage infiltration was also reduced by two distinct CCL2 antagonists, 7ND-expressing vector and propagermanium. Thus, the CCL2-CCR2 interactions regulate intracolonic infiltration of macrophages under our present conditions.

Solid tumors including colon cancers are infiltrated with leukocytes, which sometimes account for up to 50% of tumor mass, the most represented populations being lymphocytes and macrophages (37). The presence of lymphocytes is considered as

evidence of an immunologic antitumor response, whereas the presence of tumor-associated macrophages (TAM) represents a hallmark of cancer-associated inflammation (37). TAM originate from circulating monocytes that are attracted by chemotactic factors produced locally by tumor cells and resident cells. TAM produce IL-10 and transforming growth factor-β to dampen immune response to tumor cells and concomitantly promote tumor growth by producing angiogenic and growth factors. CCL2 was originally identified as a tumor-derived chemotactic factor for macrophages (38). Accumulating evidence indicates that the levels of tumor-derived CCL2 significantly correlate with TAM density and the depth of invasion in cancers of various organs (37). Moreover, experimental studies using xenotransplanted or isotransplanted tumors revealed the involvement of the CCL2-CCR2 axis in cancer invasion and metastasis (16, 39).

To clarify the roles of the CCL2-CCR2 in the progression phase of this colon carcinogenesis model, we used two different measures to

block CCL2 activity; i.m. injection of 7ND expression vector and administration of propagermanium. The biological activity of CCL2 depends on the integrity of its NH_2 terminus and 7ND, a mutant protein lacking NH_2-terminal amino acids 2 to 8, which can form a heterodimer with WT CCL2 protein (15), to suppress CCL2 activity (40). I.m. transduction of 7ND-expressing vector can result in continuous i.m. 7ND protein expression and its subsequent secretion into the circulation (41), thereby preventing CCL2-mediated tissue injuries such as vascular remodeling (41), atherosclerosis (41), and renal fibrosis after reperfusion injury (42). 7ND could effectively block CCL2 function *in vivo* and suppress inflammatory and proliferative changes in animal models of cardiovascular diseases (43), as well as in a model of renal fibrosis (44). Another CCR2 inhibitor, propagermanium, targets glycosylphosphatidylinositol-anchored proteins associated closely with CCR2, and selectively inhibits MCP-1/CCR2 signaling (45). Both measures attenuated intracolonic macrophage infiltration and neovascularization, and eventually reduced the numbers and sizes of colon carcinomas. Thus, it is reasonable to speculate that the CCL2 axis is crucially involved in the progression phase of colon carcinogenesis by regulating macrophage infiltration.

TAM can produce various factors to promote tumor growth and angiogenesis. Among them, prostaglandin E_2 (PGE_2) is presumed to be crucially involved in colon carcinogenesis because it can induce neovascularization (46) and activate a pathway crucial for colon carcinogenesis, the Wnt/β-catenin pathway, through activation of phosphoinositide 3-kinase/Akt-G protein $α_s$-axin signaling axis (47) and inhibition of glycogen synthase kinase-3 (48). COX-2 is an important enzyme in PGE_2-generating pathway and its expression is highly inducible in various types of cells including macrophages (49). COX-2 protein was detected in infiltrating F4/80-positive cells (10) and CCR2-expressing cells. Moreover, CCL2 can induce COX-2 expression in human monocytes (50). Thus, CCL2 blocking may reduce the infiltration of COX-2–expressing F4/80-positive cells and depress COX-2 expression by infiltrating macrophages, and eventually inhibit the Wnt signaling pathway and neovascularization, resulting in retardation of cancer progression.

Based on our previous observation that blocking TNF-α reversed colon carcinoma progression even after colon carcinoma was established, we proposed that drugs targeting TNF-α may be useful for the treatment of colon cancers, particularly those arising from chronic inflammation (10). Blocking CCL2 retarded colon cancer progression in this model with similar efficacy as TNF-α blockade, when given after multiple colon tumors were developed. Thus, drugs targeting CCL2 may be effective for the treatment of chronic inflammation-associated colon cancer, similarly to those targeting
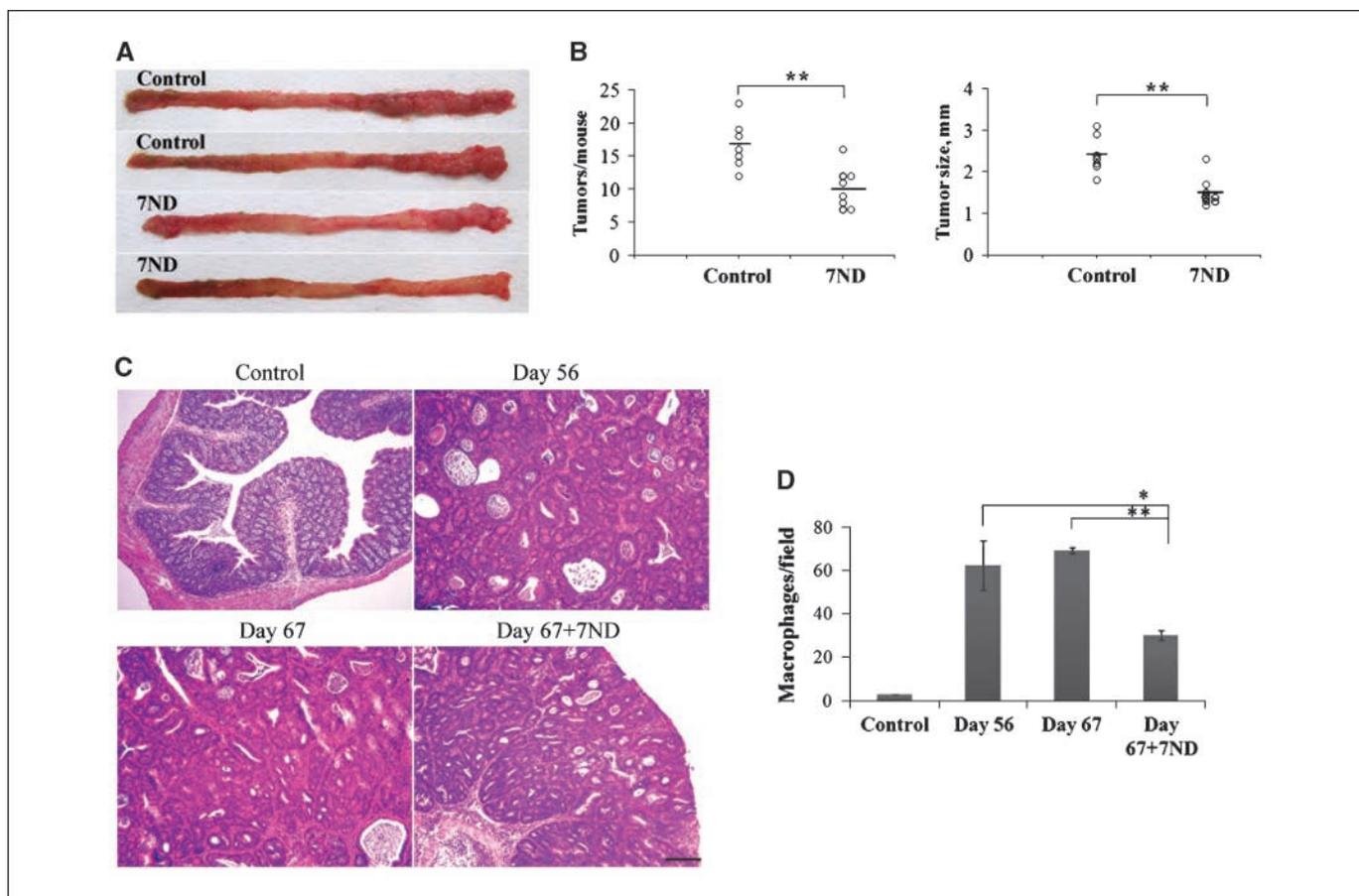

Figure 5. The effects of 7ND-expressing vector injection on colon carcinogenesis. *A,* macroscopic evaluation of the tumors. Colons were removed on day 67 from WT mice, injected with 7ND-expressing or with pcDNA3 vector. Representative results from seven to eight independent animals are shown here. *B,* the tumor numbers and sizes were determined macroscopically. *Bars,* the mean of each group. Each symbol represents the tumor numbers of each animal or the average size of the tumors of each animal. **, $P < 0.01$ versus WT mice injected with pcDNA3 vector. *C,* colons were processed to H&E staining and representative results from six independent animals are shown. *Scale bar,* 50 μm. *D,* F4/80-positive macrophages were enumerated as described in Materials and Methods. *Columns,* mean ($n = 5$ animals); *bars,* SD. *, $P < 0.05$; **, $P < 0.01$ versus WT mice injected with pcDNA3 vector.
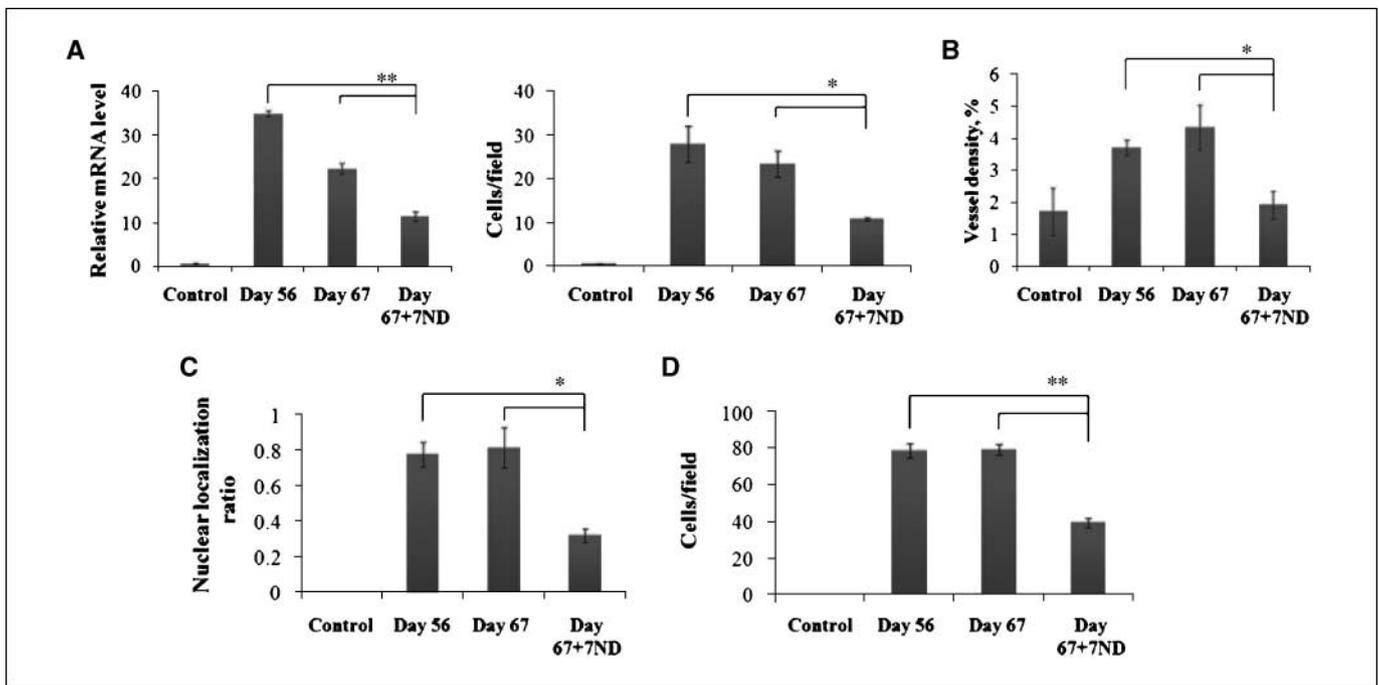
Figure 6. The effect of 7ND-expressing vector injection on colon carcinoma progression. *A,* COX-2 expression after 7ND-expressing vector injection. Quantitative RT-PCR analysis for COX-2 mRNA (*left*) and immunohistochemical analysis with anti–COX-2 antibody (*right*) were at the indicated time points as described in Materials and Methods. The levels of COX-2 mRNA were normalized to the levels of GAPDH mRNA (*left*), whereas the numbers of COX-2–expressing cells were determined on five independent animals as described in Materials and Methods (*right*). *Columns,* mean were calculated on all values; *bars,* SD. *, $P < 0.05$ versus WT mice injected with pcDNA3 vector; **, $P < 0.01$ versus WT mice injected with pcDNA3 vector. *B,* the vascular areas were determined as described in Materials and Methods. *, $P < 0.05$ versus WT mice injected with pcDNA3 vector. *C,* the β-catenin nuclear localization ratio was determined as the ratio of the numbers of tumor nuclei with β-catenin localization to the total number of tumor nuclei per field. At least five randomly chosen fields at ×400 magnification were examined. *Columns,* mean; *bars,* SD; *, $P < 0.05$ versus WT mice injected with pcDNA3 vector. *D,* the numbers of cytokeratin 20–positive cells were determined on five randomly chosen visual fields at ×400 magnification. *Columns,* mean; *bars,* SD, **, $P < 0.01$ versus WT mice injected with pcDNA3 vector.

TNF-α. Because TNF-α has a wide variety of biological functions (9), TNF-α blocking agents can have serious adverse effects including the induction of bacterial, tuberculosis, and opportunistic infection (51). CCL2 has a limited biological function, and therefore, drugs targeting CCL2 might have less severe adverse effects than those targeting TNF-α.

Disclosure of Potential Conflicts of Interest

No potential conflicts of interest were disclosed.

References

1. Fiocchi C. Inflammatory bowel disease: etiology and pathogenesis. Gastroenterology 1998;115:182–205.
2. Ullman T, Croog V, Harpaz N, Sachar D, Itzkowitz S. Progression of flat low-grade dysplasia to advanced neoplasia in patients with ulcerative colitis. Gastroenterology 2003;125:1311–9.
3. Balkwill F, Mantovani A. Inflammation and cancer: back to Virchow? Lancet 2001;357:539–45.
4. Okayasu I, Hatakeyama S, Yamada M, Ohkusa T, Inagaki Y, Nakaya R. A novel method in the induction of reliable experimental acute and chronic ulcerative colitis in mice. Gastroenterology 1990;98:694–702.
5. Okayasu I, Yamada M, Mikami T, Yoshida T, Kanno J, Ohkusa T. Dysplasia and carcinoma development in a repeated dextran sulfate sodium-induced colitis model. J Gastroenterol Hepatol 2002;17:1078–83.
6. Okayasu I, Ohkusa T, Kajiura K, Kanno J, Sakamoto S. Promotion of colorectal neoplasia in experimental murine ulcerative colitis. Gut 1996;39:87–92.
7. Greten FR, Eckmann L, Greten TF, et al. IKKβ links inflammation and tumorigenesis in a mouse model of colitis-associated cancer. Cell 2004;118:285–96.
8. Reimund JM, Wittersheim C, Dumont S, et al. Mucosal inflammatory cytokine production by intestinal biopsies in patients with ulcerative colitis and Crohn's disease. J Clin Immunol 1996;16:144–50.
9. Wang H, Czura CJ, Tracey KJ. Tumor necrosis factor. In: Thomson AW, Lotze MT, editors. The Cytokine Handbook. 4th ed. London: Elsevier Science Ltd.; 2003. p. 837–60.
10. Popivanova BK, Kitamura K, Wu Y, et al. Blocking TNF-α in mice reduces colorectal carcinogenesis associated with chronic colitis. J Clin Invest 2008;118:560–70.
11. Mazzucchelli L, Hauser C, Zgraggen K, et al. Differential *in situ* expression of the genes encoding the chemokines MCP-1 and RANTES in human inflammatory bowel disease. J Pathol 1996;178:201–6.
12. Reinecker C, Loh EY, Ringler DJ, Mehta A, Rombeau JL, MacDermott RP. Monocyte-chemoattractant protein 1 gene expression in intestinal epithelial cells and inflammatory bowel disease mucosa. Gastroenterology 1995;108:40–50.
13. Uguccioni M, Gionchetti P, Robbiani DF, et al. Increased expression of IP-10, IL-8, MCP-1 and MCP-3 in ulcerative colitis. Am J Pathol 1999;155:331–6.
14. Matsushima K, Larsen CG, DuBois GC, Oppenheim JJ. Purification and characterization of a novel monocyte chemotactic and activating factor produced by a human myelomonocytic cell line. J Exp Med 1989;169:1485–90.
15. Zhang Y, Rollins BJ. A dominant negative inhibitor indicates that monocyte chemoattractant protein 1 functions as a dimer. Mol Cell Biol 1995;15:4851–5.
16. Yang X, Lu P, Ishida Y, Kuziel WA, Fujii C, Mukaida N. Attenuated liver tumor formation in the absence of CCR2 with a concomitant reduction in the accumulation of hepatic stellate cells, macrophages and neovascularization. Int J Cancer 2006;118:335–45.
17. Wu Y, Li Y-Y, Matsushima K, Baba T, Mukaida N. CCL3–5 axis regulates intratumoral accumulation of leukocytes and fibroblasts and promotes angiogenesis in

murine lung metastasis process. J Immunol 2008;181: 6384–93.

18. Takahashi M, Wakabayashi K. Gene mutations and altered gene expression in azoxymethane-induced colon carcinogenesis in rodents. Cancer Sci 2004;95: 475–80.

19. Wong LM, Myers SJ, Tsou CL, Gosling J, Arai H, Charo IF. Organization and differential expression of the human monocyte chemoattractant protein 1 receptor gene. J Biol Chem 1997;272:1038–45.

20. Dwinell MB, Eckmann L, Leopard JD, Varki NM, Kagnoff MF. Chemokine receptor expression by human intestinal epithelial cells. Gastroenterology 1999;117: 359–67.

21. Charo IF, Myers SJ, Herman A, Franci C, Connolly AJ, Coughlin SR. Molecular cloning and functional expression of two monocyte chemoattractant protein 1 receptors reveals alternative splicing of the carboxyl-terminal tails. Proc Natl Acad Sci U S A 1994;91:2752–6.

22. Wada T, Yokoyama H, Furuichi K, et al. Intervention of crescentic glomerulonephritis by antibodies to monocyte chemotactic and activating factor (MCAF/ MCP-1). FASEB J 1996;10:1418–25.

23. Kimura H, Kasahara Y, Kurosu K, et al. Alleviation of monocrotaline-induced pulmonary hypertension by antibodies to monocyte chemotactic and activating factor/monocyte chemoattractant protein-1. Lab Invest 1998;78:571–8.

24. Moore BB, Paine R III, Christensen PJ, et al. Protection from pulmonary fibrosis in the absence of CCR2 signaling. J Immunol 2001;167:4368–77.

25. Boring L, Gosling J, Cleary M, Charo IF. Decreased lesion formation in CCR2$^{-/-}$ mice reveals a role for chemokines in the initiation of atherosclerosis. Nature 1998;394:894–7.

26. Izikson L, Klein RS, Charo IF, Weiner HL, Luster AD. Resistance to experimental autoimmune encephalomyelitis in mice lacking the CC chemokine receptor (CCR) 2. J Exp Med 2000;192:1075–80.

27. Shahrara S, Proudfoot AEI, Park CC, et al. Inhibition of monocyte chemoattractant protein-1 ameliorates rat adjuvant-induced arthritis. J Immunol 2008; 180:3447–56.

28. Guijarro LG, Mate J, Gisbert JP, et al. N-acetyl-L-cysteine combined with mesalamine in the treatment of

ulcerative colitis: randomized, placebo-controlled pilot study. World J Gastroenterol 2008;14:2851–7.

29. Andreas PG, Beck PL, Mizoguchi E, et al. Mice with a selective deletion of the CC chemokine receptors 5 or 2 are protected from dextran sodium sulfate-mediated colitis: lack of CC chemokine receptor 5 expression results in a NK1.1$^+$ lymphocyte-associated Th2-type immune response in the intestine. J Immunol 2000;164: 6303–12.

30. Salcedo R, Ponce ML, Young HA, et al. Human endothelial cells express CCR2 and respond to MCP-1: direct role of MCP-1 in angiogenesis and tumor progression. Blood 2000;96:34–40.

31. Carulli MT, Ong VH, Ponticos M, et al. Chemokine receptor CCR2 expression by systemic sclerosis fibroblasts: evidence for autocrine regulation of myofibroblast differentiation. Arthritis Rheum 2005;52:3772–82.

32. Klopp AH, Spaeth EL, Dembinski JL, et al. Tumor irradiation increases the recruitment of circulating mesenchymal stem cells into the tumor microenvironment. Cancer Res 2007;67:11687–95.

33. Lu Y, Cai Z, Galson DL, et al. Monocyte chemotactic protein-1 (MCP-1) acts as a paracrine and autocrine factor for prostate cancer growth and invasion. Prostate 2006;66:1311–8.

34. Spring H, Schuler T, Arnold B, Hammerling G, Ganss R. Chemokines direct endothelial progenitors into tumor neovessels. Proc Natl Acad Sci U S A 2005; 102:18111–6.

35. Moore BB, Kolodsick JE, Thannickal VJ, et al. CCR2-mediated recruitment of fibrocytes to the alveolar space after fibrotic injury. Am J Pathol 2005;166:675–84.

36. Tokuyama H, Ueha S, Kurachi M, et al. The simultaneous blockade of chemokine receptors CCR2, CCR5 and CXCR3 by a non-peptide chemokine receptor antagonist protects mice from dextran sodium sulfate-mediated colitis. Int Immunol 2005;17:1023–34.

37. Sica A, Allavena P, Mantovani A. Cancer related inflammation: the macrophage connection. Cancer Lett 2008;264:204–15.

38. Graves DT, Jiang YL, Williamson MJ, Valente AJ. Identification of monocyte chemotactic activity produced by malignant cells. Science 1989;245:1490–3.

39. Loberg RD, Ying C, Craig M, et al. Targeting CCL2 with systemic delivery of neutralizing antibodies

induces prostate cancer regression *in vivo*. Cancer Res 2007;67:9417–24.

40. Gong JH, Clark-Lewis I. Antagonists of monocyte chemoattractant protein 1 identified by modification of functionally critical NH$_2$-terminal residues. J Exp Med 1995;181:631–40.

41. Kitamoto S, Egashira K. Anti-monocyte chemoattractant protein-1 gene therapy for cardiovascular diseases. Expert Rev Cardiovasc Ther 2003;1:393–400.

42. Furuichi K, Wada T, Iwata Y, et al. Gene therapy expressing amino-terminal truncated monocyte chemoattractant protein-1 prevents renal ischemia-reperfusion injury. J Am Soc Nephrol 2003;14:1066–71.

43. Kitamoto S, Egashira K. Gene therapy targeting monocyte chemoattractant protein-1 for vascular disease. J Atheroscler Thromb 2002;9:261–5.

44. Wada T, Furuichi K, Sakai N, et al. Gene therapy via blockade of monocyte chemoattractant protein-1 for renal fibrosis. J Am Soc Nephrol 2004;15:940–8.

45. Yokochi S, Hashimoto H, Ishiwata Y, et al. An anti-inflammatory drug, propagermanium, may target GPI-anchored proteins associated with an MCP-1 receptor, CCR2. J Interferon Cytokine Res 2001;21:389–98.

46. Iniguez MA, Rodriguez A, Volpert OV, Fresno M, Redondo JM. Cyclooxygenase-2: a therapeutic target in angiogenesis. Trends Mol Med 2003;9:73–8.

47. Castellone MD, Teramoto H, Williams BO, Druey KM, Gutkind JS. Prostaglandin E$_2$ promotes colon cancer cell growth through a G$_s$-axin-β-catenin signaling aixs. Science 2005;310:1504–10.

48. Shao J, Jung C, Liu C, Sheng H. Prostaglandin E$_2$ stimulates the β-catenin/T cell factor-dependent transcription in colon cancer. J Biol Chem 2005;280: 26565–72.

49. Arias-Negrete S, Keller K, Chadee K. Proinflammatory cytokines regulate cyclooxygenase-2 mRNA expression in human macrophages. Biochem Biophys Res Commun 1995;208:582–9.

50. Tanaka S, Tatsuguchi A, Futagami S, et al. Monocyte chemoattractant protein 1 and macrophage cyclooxygenase 2 expression in colonic adenoma. Gut 2006;55: 54–61.

51. Rutgeerts P, Sandborn WJ, Feagan BG, et al. Infliximab for induction and maintenance therapy for ulcerative colitis. N Engl J Med 2005;353:2462–76.

Cancer Research

The Journal of Cancer Research (1916–1930) | The American Journal of Cancer (1931–1940)

AAC⬡R American Association for Cancer Research

Blockade of a Chemokine, CCL2, Reduces Chronic Colitis-Associated Carcinogenesis in Mice

Boryana Konstantinova Popivanova, Feodora Ivanova Kostadinova, Kengo Furuichi, et al.

Cancer Res 2009;69:7884-7892. Published OnlineFirst September 22, 2009.

Updated version	Access the most recent version of this article at: doi:10.1158/0008-5472.CAN-09-1451
Supplementary Material	Access the most recent supplemental material at: http://cancerres.aacrjournals.org/content/suppl/2009/09/10/0008-5472.CAN-09-1451.DC1

Cited articles	This article cites 50 articles, 21 of which you can access for free at: http://cancerres.aacrjournals.org/content/69/19/7884.full#ref-list-1
Citing articles	This article has been cited by 15 HighWire-hosted articles. Access the articles at: http://cancerres.aacrjournals.org/content/69/19/7884.full#related-urls

E-mail alerts	Sign up to receive free email-alerts related to this article or journal.
Reprints and Subscriptions	To order reprints of this article or to subscribe to the journal, contact the AACR Publications Department at pubs@aacr.org.
Permissions	To request permission to re-use all or part of this article, use this link http://cancerres.aacrjournals.org/content/69/19/7884. Click on "Request Permissions" which will take you to the Copyright Clearance Center's (CCC) Rightslink site.